Stress analysis of manufacturing processes for solar modules

Sascha Dietrich, **Matthias Pander**, **Martin Sander**, **Rico Meier** & **Matthias Ebert**, Fraunhofer Center for Silicon Photovoltaics CSP, Halle (Saale), Germany

ABSTRACT

Cracking of solar cells is a serious issue for product safety and module performance. Cracks may result in power loss, hot spots or arcing, and are caused by exceeding the strength limit of silicon. During the last few years, various studies have shown that fracture of encapsulated solar cells can be influenced by the manufacturing processes, which lead to residual stresses in solar cells. The results presented in this paper will give insights into the stresses generated by soldering and lamination. Furthermore, mechanisms of stress generation will be explained. On the basis of these findings, recommendations are made as to how to mitigate stresses, for example by means of alternative soldering processes, different soldering parameters or material optimization of the copper ribbon or the encapsulant.

Introduction

Fracture of solar cells has been identified as one of the most frequent failures in solar modules – it can lead to power loss over time as well as safety issues because of arcing or hot spots [1–3]. Furthermore, cell cracks are related to the presence of snail trails [4], which is an optical blemish on solar modules. Fracture is a mechanical issue related to mechanical stresses, which are caused by temperature changes or mechanical loads, and will occur when a certain stress limit for a material is reached. Therefore, in order to reduce crack initiation in solar cells, it is necessary to study single loads as well as load histories (during both manufacturing and operation) and how they form stresses. By means of such an approach, mechanisms can be understood, critical parameters identified, and measures derived in order to mitigate crack formation. For a deep understanding of the mechanical conditions in a PV module during manufacturing and operation, a combination of finite-element analysis and experiments under well-known conditions were performed.

> "To reduce crack initiation in solar cells, it is necessary to study single loads as well as load histories and how they form stresses."

Mechanically induced loads can be static (wind, snow) or dynamic (shock, vibration, wind gusts). Loads from temperature changes occur during manufacturing (soldering, lamination) or operation (seasons, day/night shift). It is known that thermomechanically induced stresses often lead to residual stresses, which may remain in the material; these will add to any additional stresses, such as from mechanical loading. In the case of mechanical loading, the properties of the polymeric encapsulant in the module laminate significantly influence the level of induced stress [5].

Thermomechanically induced stress is caused by a mismatch of the coefficients of thermal expansion (CTE) of materials that are bonded together. Table 1 lists typical properties of materials used in PV modules: it can be clearly seen that there are large differences in CTE as well as stiffness (Young's modulus) between the respective materials. In particular, the CTE mismatches between silicon, copper and the metallization pastes are of great importance. Since in solar module laminates the whole stack is bonded, residual stress can be expected.

Finite-element set-up

Parameterized finite-element models for cells, mini-modules and complete solar modules have recently been developed: these models comprise all material and structural components of a solar module (cells, polymers, interconnectors, frame). Figs. 1 and 2 show a portion of a model for a complete solar module. Specific material behaviour was implemented

Material	CTE at 20°C [10^{-6} K^{-1}]	Young's modulus at 20°C [GPa]
Silicon [6–8]	2.60	130–180
Copper [9]	16.65	86
Solder alloy (Sn94.5Ag4Cu0.5) [10]	22.00	40
Al paste [11–13]	15.90	6
Ag paste [9,12,14]	10.40	7
Glass [15]	8.50	63–70
EVA	300.00	1–100MPa
Backsheet	67.00	2.1

Table 1. Material properties of typical materials used in solar module laminates.

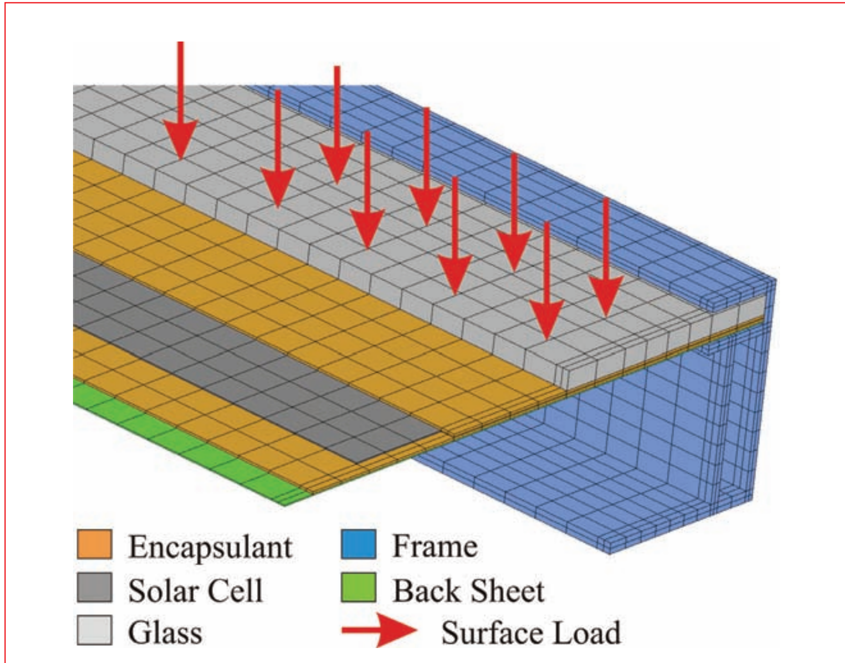

Figure 1. Portion of a finite-element model of a solar module, with a distributed surface load.

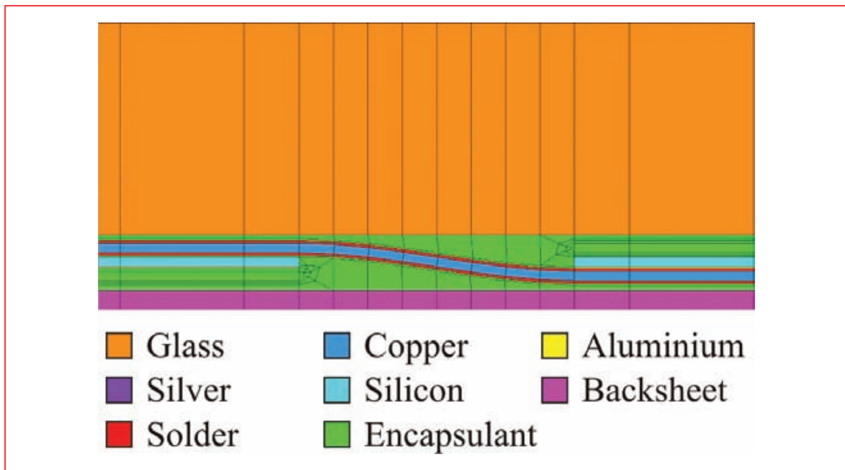

Figure 2. Detail of the finite-element model of a mini-module at the cell gap (cross section).

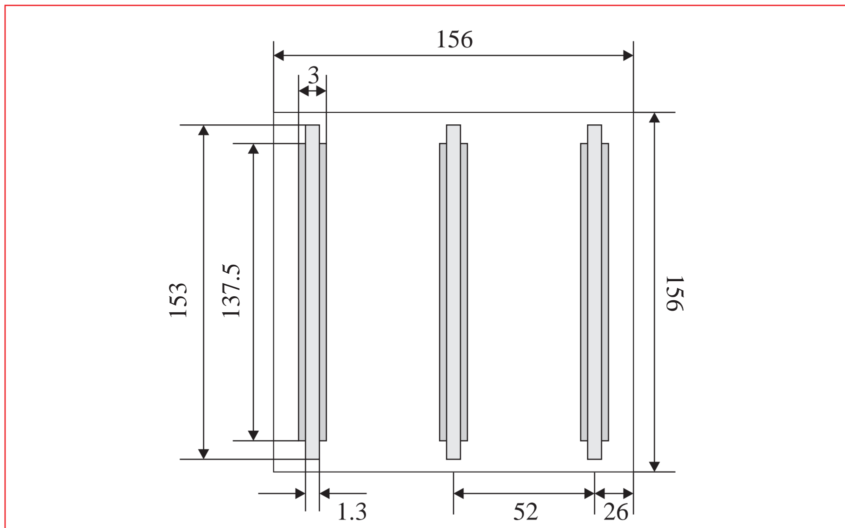

Figure 3. Cell layout used in this investigation.

in the simulation as realistically as possible. Glass and silicon were modelled by means of a linear-elastic-material model. Because polymers demonstrate a distinct time-dependent behaviour, a viscoelastic model represented by Prony series was used in this case. In the case of metallization pastes, aluminium, interconnectors and solder bonds, an elastic-plastic material behaviour was assumed. Furthermore, creep for the solder was taken into account by means of a power law behaviour.

Finite-element modelling allows the simulation of loads arising from temperature changes as well as from mechanical loads, and the calculation of strains or stresses in all components. Fig. 3 shows the layout of the solar cell used in the investigations reported in this paper: it consists of three busbars, with front and back contacts and continuous busbars.

Experiments

Experiments were carried out on representative laminates consisting of 10 solar cells (two strings each with five cells). The test set-up, test procedure and evaluation are presented in Fig. 4. A four-point bending set-up is used, in which the laminate is placed with the cells sunny-side upwards. Load steps of 10N increments are applied to the laminate. For each step, an electroluminescence (EL) image is taken from the cells between the load rollers, which allows the determination of cell cracking with respect to stress direction and finally of the in-laminate strength of solar cells. More details about the experimental approach can be found in Sander et al. [16]. The result of this test is a value for the effective strength of the encapsulated solar cells, where all previous steps from manufacturing (introduced defects through processing, residual stresses) are included. For the evaluation, all cells are assumed to be stress free; this allows influences to be recognized by a change in fracture force or fracture strength.

> "Process parameters during soldering may influence the in-laminate fracture strength of solar cells."

For the experimental studies, cell strings with two different soldering techniques (laser, infrared) and

SCHMID

Imagine You'd Save as Much Silver to Plate the Eiffel Tower...

September 23th to 25th 2014
Amsterdam, Netherlands
Booth C6, Hall 1

Expect Solutions. **TinPad.**

Eliminate the need of silver on cell backsides and increase efficiency at the same time. TinPad is a really simple way to apply tin busbars with best adhesion. In a highly competitive market, this tool is a must-have to reduce costs in the short term and a get long ranging profit increase.

In a cell production line with a throughput of 2.200 wph, 95% uptime and 50mg Ag backside consumption you would save as much silver in one year to cover an area of over 275000m² with 1μm leaf silver. That's more than enough to plate the Eiffel Tower. Or to simply increase your profit.

150 YEARS SCHMID Expect Solutions

www.schmid-group.com/tinpad

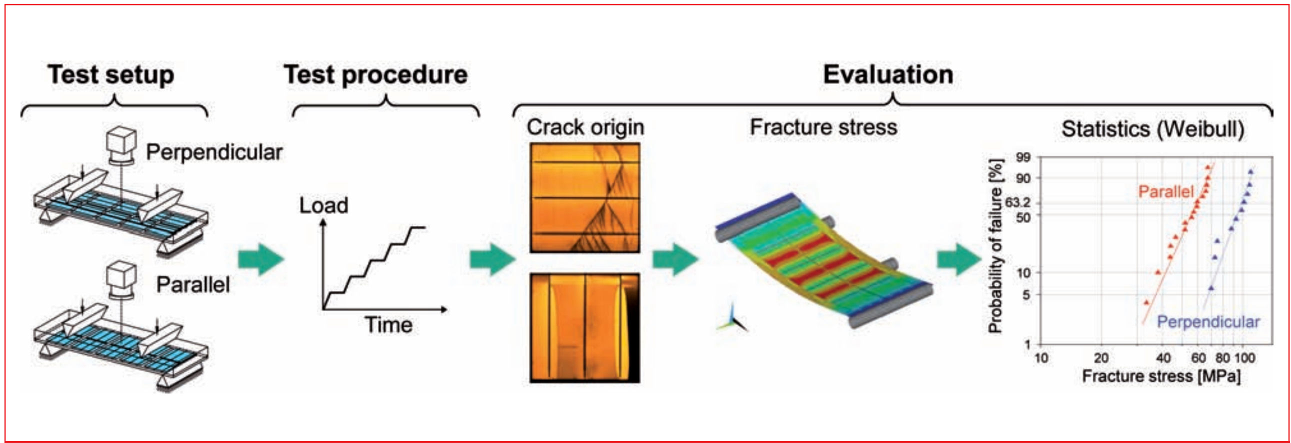

Figure 4. Experimental approach for in-laminate strength testing of solar cells [5].

process parameters were produced and laminated. For each technique and parameter set, laminates were produced with a stiff and a soft EVA encapsulant; they were then subjected to in-laminate strength testing, giving the results shown in Fig. 5. It can be seen that process parameters during soldering may influence the in-laminate fracture strength of solar cells (especially infrared soldering); this correlates with previous results [17]. However, for laser soldering, no major influence of process parameters could be found, which may imply a robust technology with a wider process window. If the two process techniques are compared, a statistically significant difference can be found when lower temperatures are used with a longer duration: the differences, however, are fairly small.

Also included in this investigation was a comparison of two EVA encapsulants having different stiffness properties. Depending on the composition of the EVA, especially the VA content, stiffness can be adjusted by moving the glass transition to higher or lower temperatures. The results show that a soft EVA leads to higher in-laminate strength values, implying that a module would resist higher loads (Fig. 5).

During the experiments it can be asserted that crack initiation often occurs at the busbars (see Fig. 6); this can also be observed on complete modules, where cracks often start at the end of the busbars or along them. In addition, cracks often propagate along the busbars [18]. In order to understand the reason for this, the manufacturing processes need to be considered. The soldering and lamination processes have therefore both been simulated in order to analyse stress distribution in the silicon.

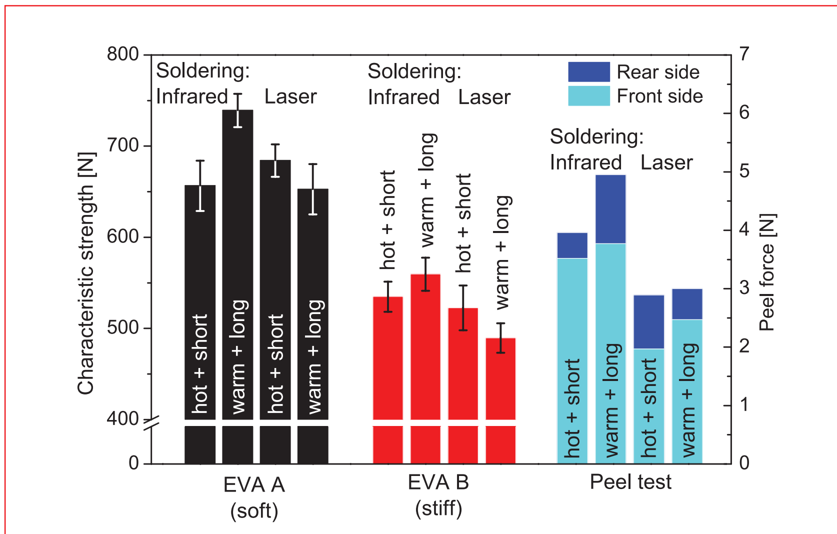

Figure 5. Measured in-laminate fracture strength/force of specimens produced under different manufacturing conditions, and the results of the peel test of the soldered cells for the different soldering conditions [5]. (The error bars are the confidence intervals for a confidence level of 95%.)

Figure 6. EL image of broken cells after in-laminate strength testing [5].

Stress analysis of soldering processes

The first temperature-driven process during module production is the fabrication of cell strings; temperatures up to 240°C can be reached, depending on the composition of the solder. Besides the metallurgical aspects, the solidus temperature differentiates types of solder. This is of particular interest since, along with material properties, it defines the temperature difference ΔT from room temperature. Typical solidus temperatures are between 180 and 220°C, but some special solders, such as tin/bismuth, have even lower solidus temperatures of around 130°C.

Since materials with different coefficients of thermal expansion

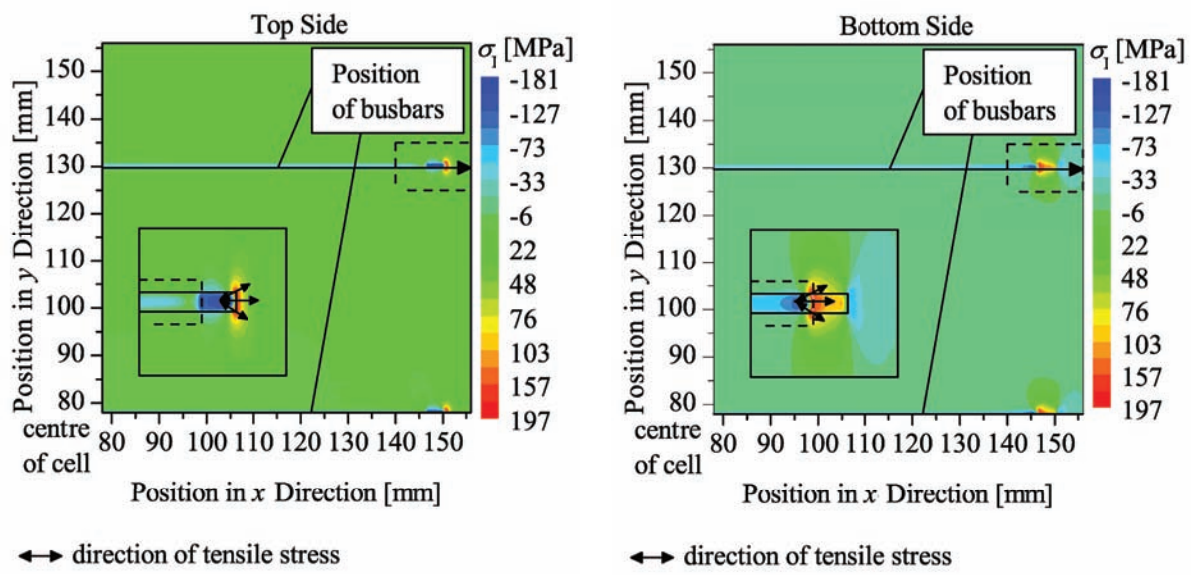

Figure 7. First principal stress in the silicon after soldering (only a quarter of a cell is shown for reasons of symmetry).

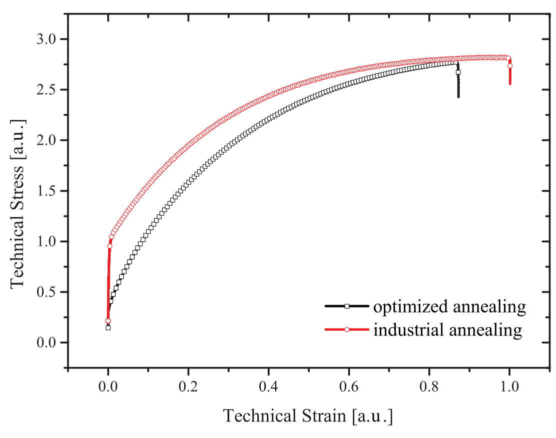

Figure 8. Tensile testing results for a standard industrial interconnector and an optimized interconnector [19].

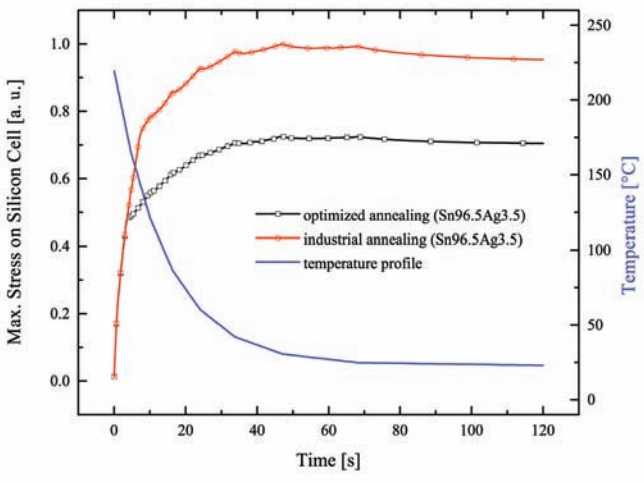

Figure 9. Maximum stress during the cooling phase of the soldering process for a standard industrial interconnector and an optimized interconnector [19].

are bonded together, stresses are developed in each material. In the case of ductile materials – such as solder, copper or the silver pastes – the increase in stress is lower because of plastic deformation and hardening, which is an important aspect that will be discussed later. However, silicon does not have this quality, since it is a linear elastic material within the respective temperature ranges of module manufacturing and operation. Stresses therefore increase with a steady gradient until brittle fracture occurs.

Simulations have been carried out with a solder (SnAg4Cu0.5) that has a solidus temperature of 217°C: this temperature represents the stress-free state in the performed simulation. A single solar cell was cooled to 25°C within 60 sec. Fig. 7 shows the stress distribution on the top and bottom surfaces of the solar cell: the influence at the busbars can be clearly seen. Pressure stresses are developed underneath the busbar, which is in accordance with mechanical principles, since copper and metallization pastes have a higher CTE than silicon. As a consequence, stress peaks can be found at the end of the soldered busbar on both the top and bottom sides. The arrows in Fig. 7 indicate the direction of the first principal stress. It is directed in a perpendicular direction to the perimeter of the soldered area, which is an important fact since any additional stress – for example from lamination or later module bending – has to be oriented in the same direction in order that a constructive or destructive superimposition can take place.

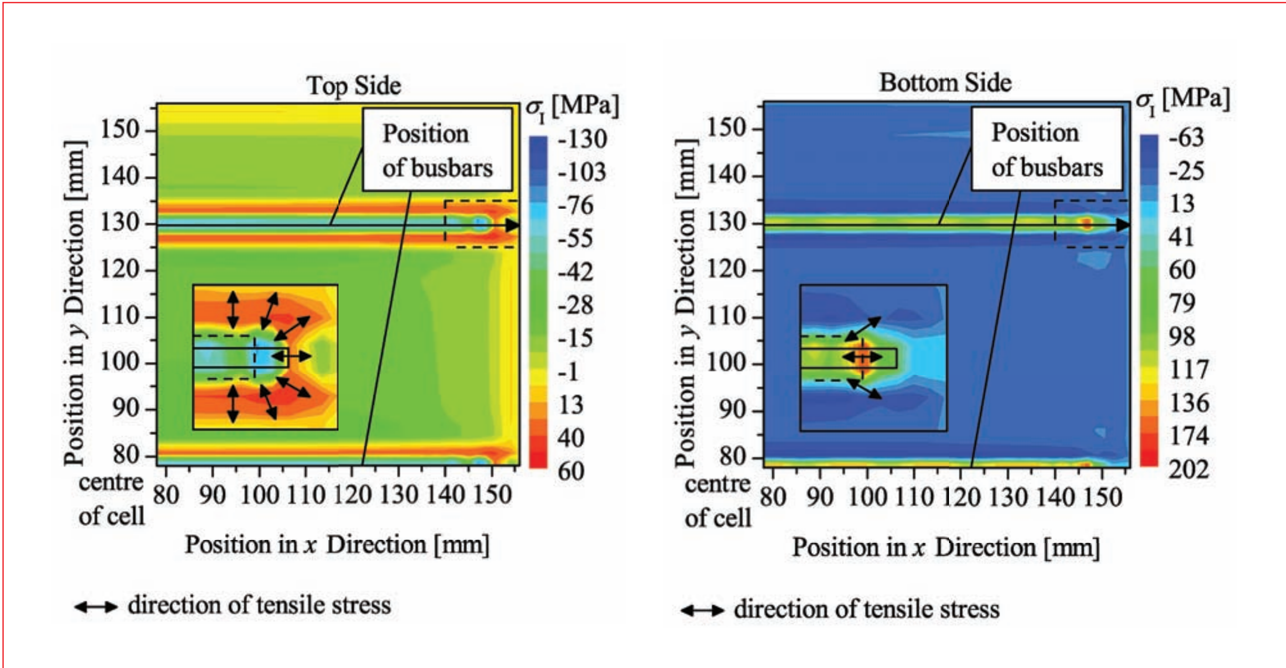

Figure 10. First principal stress in the silicon after lamination (only a quarter of a cell is shown for reasons of symmetry).

Optimized interconnectors for reducing mechanical stresses from soldering

The experimental studies discussed above showed that the soldering technique and process parameters do not necessarily have a large impact on cell reliability. Material properties, however, may have an influence. Interconnectors are produced from copper material in order to achieve a low series resistance at an acceptable cost. As described above (Table 1), the CTE of copper is about six times as large as that of silicon, which is one of the main reasons for stress evolution in solar cells. The magnitude of this stress is mostly limited by the yield strength and the strain hardening properties of the copper; basically, yield strength should be as low as possible. Meier et al. [19] investigated how the yield strength of copper ribbons can be reduced by annealing. In Fig. 8 the yield strength of a standard industrial interconnector was reduced by changes to the annealing process.

> "Yield strength should be as low as possible."

An elastic-plastic material model was used in order to transfer the experimental data to the finite-element model. Fig. 9 shows the result for the evolution of the maximum first principal stress in the silicon during cooling: it can be clearly seen that the reduced yield strength leads to a stress reduction in the silicon.

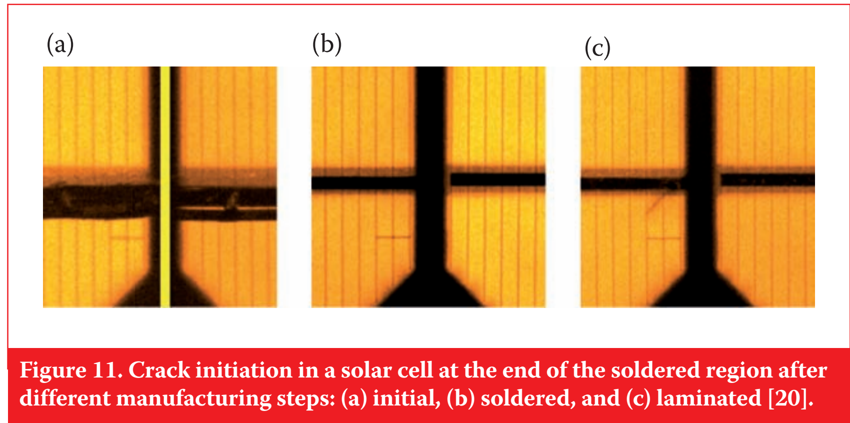

Figure 11. Crack initiation in a solar cell at the end of the soldered region after different manufacturing steps: (a) initial, (b) soldered, and (c) laminated [20].

Stress analysis of the lamination process

After the soldering process, cell strings are placed on a glass pane between two layers of encapsulant. In a first step the laminate stack is heated up to lamination temperature (around 150°C); during this heating, the laminate compound is assumed to be not bonded, so the cells are able to move freely. The heating step is included in the simulation immediately after cooling from the soldering temperature. This is important since copper is deformed plastically during these large temperature changes, which influences the outcome of the stress calculation. After being heated up to lamination temperature, all materials are defined to be bonded, and the laminate is cooled down to room temperature within 50 min (in-house measurements at Fraunhofer CSP).

Fig. 10 illustrates the calculated first principal stress distribution on the surfaces of the silicon after lamination: it is obvious that there are major differences between the top and bottom sides of the cell. On the top side, pressure stress can be found underneath the busbars; in contrast, on the bottom side, tensile stress is created, which exceeds the intrinsic compressive stress from soldering. At the sides of the busbars, the opposite is true: there is tensile stress on the top side, whereas there is pressure stress on the bottom.

A lamination stress peak similar to the one in the case of soldering can be found at the end of the soldered region on the bottom side of the cell. The direction of the stress correlates with that caused by soldering. As a result, stresses from soldering and lamination will superimpose and, in this case, accumulate at this position, leading to a higher probability of fracture.

Qualitatively similar stress results can be found on the top side at the end of the busbar.

> "Stresses from soldering and lamination will superimpose, leading to a higher probability of fracture."

Sander et al. [20] investigated cell fracture for each manufacturing step of small cell strings. Fig. 11 shows EL images in the initial state of two adjacent solar cells, after soldering and lamination. Typically, it was discovered that there is a high likelihood of crack initiation during lamination at the end of the busbar, which usually corresponds to the end of the soldered length. This correlates well with the observations in the stress analysis.

Fig. 12 shows the exaggerated deformed finite-element mesh from a portion of the perpendicular cross section through the busbar. This deformation plot is extracted after cooling down from the lamination temperature to 20°C, and shows that the main mechanism of stress generation is the contraction of the encapsulant during cooling. Since the solar cell is bonded to the glass via the encapsulant, the contraction of the latter pulls it to the glass. The distance between the copper ribbon and the glass is smaller than the distance between the surface of the cell and the glass, since the polymer is squeezed out during lamination. Measurements taken of some samples showed that the distance between the glass and the copper ribbon is 160–170µm, whereas the distance between the cell and the glass is approximately 400µm. Since the relative contraction of the polymer is the same at any point, the absolute contraction is determined by the initial thickness of the polymer. Thus the absolute contraction between the cell and the glass is larger than that between the ribbon and the glass. Contractions of 60µm between the cell and the glass, and 14µm between the ribbon and the glass, were determined from the simulation. Furthermore, pressure stresses were created between the busbars, because the contraction of the glass was larger than that of silicon.

Finite-element simulation on full-scale modules

Finite-element simulation models of complete modules were used for investigations of full-scale modules. A distributed load of 2400Pa, in accordance with the IEC standard for testing against wind loads, was applied to the glass surface of the module, which was defined to be supported along its long perimeter. Fig. 13 shows a contour plot of the first principal stress of the encapsulated solar cells; the stress which is applied by mechanical bending is shown in Fig. 13(a). High stresses, which increase the likelihood of cell breakage, can be expected in the corner cells and in the cells in the centre of the module, with maximum stresses ranging between 40 and 50MPa. However, this stress distribution will change if the position of the support is moved (as shown by Dietrich et al. [21]) or if the load changes.

In Fig. 13(b) the intrinsic stresses from manufacturing are superimposed with stresses from bending. Very localized stress peaks are created along the busbars, increasing the maximum stress to 93MPa. Moreover, the magnitude of the stress between the busbars is reduced because of the pressure stress that is applied during lamination, implying that fracture will more likely start from the busbars.

Summary

Experimental and simulation studies showed that cracks in solar cells are likely to start along the busbars of solar cells.

- Maximum production yields
- Optimum module efficiency
- Long-term module reliability

For even greater value, ALPHA PV Ribbon comes "pre-fluxed" – ask us about ALPHA PV Ready Ribbon.

Connect with ALPHA PV Ribbon at for more information.

alpha
PV Technologies

Worldwide/Americas Headquarters
300 Atrium Drive • Somerset, NJ 08873 USA
+1-800-367-5460

European Headquarters • Forsyth Road
Sheerwater • Woking GU215RZ • United Kingdom
+44-1483-758-400

Asia-Pacific Headquarters • 8/F, Paul Y. Centre
51 Hung To Road • Kwun Tong
Kowloon, Hong Kong • +852-3190-3100

© 2014 Alpha

These cracks may be either initiated during manufacturing (most likely during lamination) or a result of bending caused by a mechanical load (wind or snow) on a solar module. Since several materials with very different material properties, and in particular different coefficients of thermal expansion, are bonded together, they will contract or expand differently during temperature changes, causing stresses in each material component. Because of the brittle characteristic of silicon, fracture occurs suddenly without any previous indication of overload. Numerical studies have shown that high local stress peaks are induced in the silicon around the busbars. As a result of plastic deformation, materials such as metal pastes, solder and copper ribbons can limit the stress. These types of material can therefore also be optimized to limit the stress in the solar cell, which can be achieved, for example, by optimizing yield strength.

> "Cracks in solar cells are likely to start along the busbars of solar cells."

Furthermore, lamination turns out to be rather critical as regards the fracture of solar cells: experimental studies have shown that this manufacturing step has the highest probability of initiating cracks, and numerical studies have confirmed these observations. Stresses from soldering and lamination add together on the basis of the same mechanism (temperature change and CTE mismatch). A second mechanism was found to be the bending of the solar cell around the busbar caused by the contraction of the encapsulant. This bending gives rise to high stress peaks in a relatively large area around the busbar. Therefore, alternative polymers (such as a silicone-based material with a lower CTE), a different lamination profile, or a lower stiffness can all reduce those stresses.

Residual stresses generated in the manufacturing chain remain in the silicon. Although viscoelastic effects of the polymers involved and solder may reduce some of those stresses over time (creeping), the effect decreases as the stresses become smaller, so that after a while a non-diminishing stress minimum is reached. Therefore intrinsic stresses from manufacturing are present in a module and will superimpose with stresses from additional mechanical loads or from loads due to temperature changes, which dominate the fracture of an encapsulated solar cell, as numerical studies demonstrate. Simulation results from lamination showed that a region of high tensile stresses is present along the busbar, and these stresses are directed in a perpendicular direction to the busbar. As a consequence, it is likely that cracks will propagate closely along the busbar; this correlates with results from module EL imaging as well as in-laminate strength tests when stress from bending is also perpendicular to the busbars [16].

Finally, it can be stated that systematic experimental studies in combination with sophisticated numerical simulation can contribute to a comprehensive knowledge about fracture mechanisms in solar cells. Interpretations can be made in order to optimize a solar module in terms of mechanical reliability. However, these interpretations are individual, as they are limited by certain constraints (such as the processes that are currently

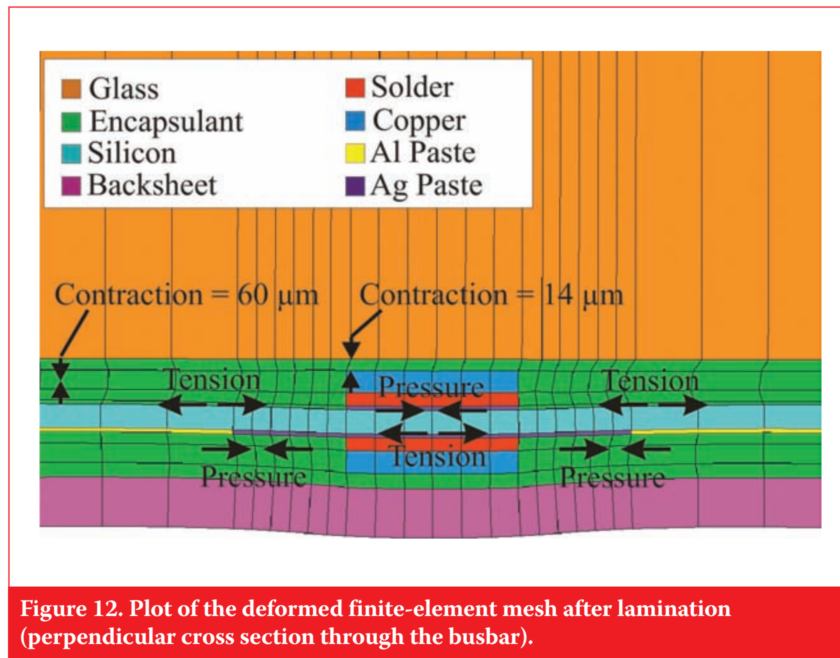

Figure 12. Plot of the deformed finite-element mesh after lamination (perpendicular cross section through the busbar).

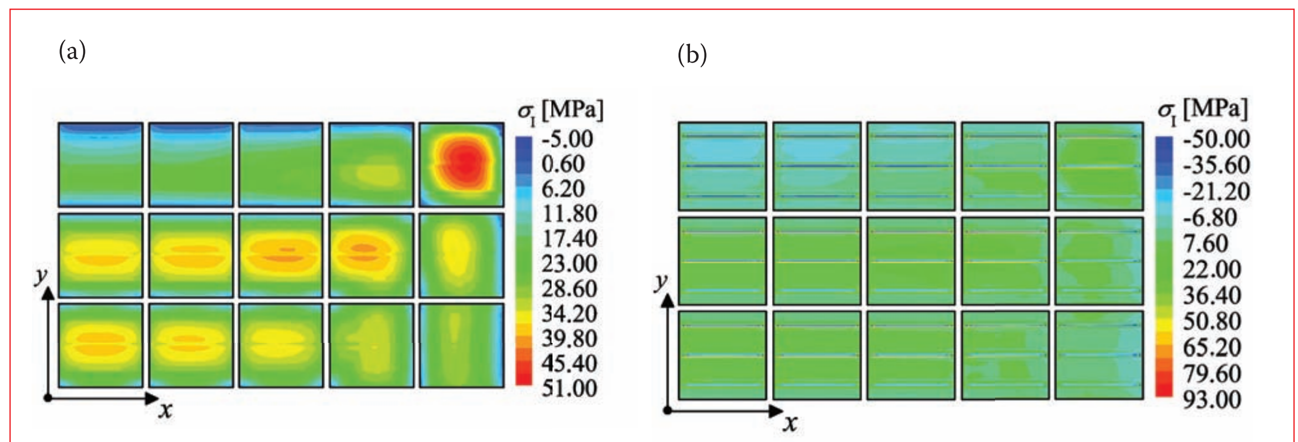

Figure 13. First principal stress plot of encapsulated solar cells at 2400Pa supported along the long perimeter of the module: (a) stress due only to mechanical bending; (b) superimposition of stresses from soldering, lamination and bending.

used for module production) or design restrictions.

References

[1] Koentges, M. et al. 2011, "The risk of power loss in crystalline silicon based photovoltaic modules due to micro-cracks", *Solar Energy Mater. & Solar Cells*, Vol. 95, pp. 1131–1137.

[2] Wohlgemuth, J. et al. 2011, "Reliability testing beyond qualification as a key component in photovoltaic's progress toward grid parity", *Proc. IEEE Intl. Rel. Phys. Symp.*, Monterey, California, USA, pp. 5E.3.1–5E.3.6.

[3] Wohlgemuth, J. et al. 2006, "Long term reliability of PV modules", *Proc. 4th IEEE WCPEC*, Waikoloa, Hawaii, USA, pp. 2050–2053.

[4] Ezquer, M. 2013, "Characterization defects detected on c-Si PV modules after certain period of field exposure", *Proc. 28th EU PVSEC*, Paris, France, pp. 3269–3274

[5] Sander, M. et al. 2013, "Influence of manufacturing processes and subsequent weathering on the occurrence of cell cracks in PV modules", *Proc. 28th EU PVSEC*, Paris, France, pp. 3275–3279.

[6] Hull, R. (Ed.) 1999, *Properties of Crystalline Silicon*. London: INSPEC, The Institution of Electrical Engineers.

[7] Okada, Y. et al. 1984, "Precise determination of lattice parameter and thermal expansion coefficient of silicon between 300 and 1500 K", *J. Appl. Phys.*, Vol. 56, pp. 314–320.

[8] Okaji, M. 1988, "Absolute thermal expansion measurements of single-crystal silicon in the range 300–1300 K with an interferometric dilatometer", *Intl. J. Thermophys.*, Vol. 9, pp. 1101–1109.

[9] Chang, Y.A. et al. 1966, "Temperature dependence of the elastic constants of Cu, Ag, and Au above room temperature", *J. Appl. Phys.*, Vol. 37, pp. 3567–3572.

[10] Wiese, S. et al. 2002, "Characterisation of constitutive behaviour of SnAg, SnAgCu and SnPb solder in flip chip joints", *Sens. and Act. A*, Vol. 99, pp. 188–193.

[11] Brandes, E.A. & Brook, G.B. (Eds.) 1983, *Smithells Metals Reference Book*, 6th edn. Oxford: Butterworth-Heinemann.

[12] Kohn, C. et al. 2007, "Analyses of warpage effects induced by passivation and electrode coatings in solar cells", *Proc. 22nd EU PVSEC*, Milan, Italy.

[13] Tallon, J.L. et al. 1979, "Temperature dependence of the elastic constants of aluminium", *J. Phys. Chem. Solids*, Vol. 40, pp. 831–837.

[14] Smith, D.R. et al. 1995, "Low-temperature properties of silver", *J. Res. Natl. Inst. Stand. Technol.*, Vol. 10, pp. 119–171.

[15] Scholze, H. 1988, *Glas – Natur, Struktur und Eigenschaften* (in German), 3rd edn. Berlin: Springer Verlag.

[16] Sander, M. et al. 2013, "Systematic investigation of cracks in encapsulated solar cells after mechanical loading", *Solar Energy Mater. & Solar Cells*, Vol. 111, pp. 82–89.

[17] Gabor, A.M. et al. 2006, "Soldering induced damage to thin solar cells and detection of cracked cells in modules", *Proc. 21st EU PVSEC*, Dresden, Germany.

[18] Koentges, M. et al. 2011, "Crack statistics of crystalline silicon photovoltaic modules", *Proc. 26th EU PVSEC*, Hamburg, Germany, pp. 3290–3294.

[19] Meier, R. et al. 2011, "Reduction of soldering induced stresses in solar cells by microstructural optimization of copper-ribbons", *Proc. SPIE*, San Diego, USA, pp. 811206-1–811206-13.

[20] Sander, M. et al. 2011, "Investigations on crack development and crack growth in embedded solar cells", *Proc. SPIE*, San Diego, USA, pp. 811209-1–811209-10.

[21] Dietrich, S. et al. 2012, "Interdependency between mechanical failure rate of encapsulated solar cells and module design parameters", *Proc. SPIE*, San Diego, USA, pp. 84720P-1–84720P-9.

About the Authors

Sascha Dietrich studied mechanical engineering at the University of Applied Sciences Leipzig and at the University of Paisley in Scotland. Since 2008 he has been working in the module reliability group at Fraunhofer CSP. Currently he is head of the lifetime and weathering team, which is responsible for lifetime testing of PV modules and components. During this time, he worked on his Ph.D., with a thesis topic involving numerical studies of the mechanical reliability of encapsulated solar cells.

Matthias Pander studied mechanical engineering at the University of Applied Sciences Leipzig. His master's thesis involved the simulation of the thermomechanical stresses in embedded solar cells. Since 2010 he has been working in the module reliability group at the Fraunhofer CSP, focusing on material characterization and finite-element simulations for components of photovoltaic modules.

Martin Sander studied mechanical engineering in Ilmenau, Germany, and received his diploma in 2008. He then worked in the module reliability group at Fraunhofer CSP, where he completed his Ph.D. thesis on the investigation of cracks in encapsulated solar cells during thermal and mechanical loads. He recently joined TOTAL New Energies and works in solar R&D.

Rico Meier studied in the International Physics Studies Program at Leipzig University. In his master's thesis, he addressed the influence of mechanical stress and temperature on the ultrasonic time of flight in solid objects. Since January 2009, he has been working with the module reliability group at Fraunhofer CSP, where he specializes in the ultrasonic characterization of solar cell interconnectors in crystalline PV modules.

Matthias Ebert is head of the module reliability group at Fraunhofer CSP in Halle (Saale), Germany. He studied civil engineering at the Bauhaus University Weimar and received his Ph.D. from the Institute for Structural Mechanics in Weimar. He began working at Fraunhofer Institute for Mechanics of Materials in 2003, and has been at Fraunhofer CSP since 2007.

Enquiries

Sascha Dietrich
Fraunhofer Center for Silicon Photovoltaics CSP
Otto-Eissfeldt-Str. 12
06120 Halle (Saale)
Germany

Tel: +49 (0) 345 5589 5210
Email: sascha.dietrich@csp.fraunhofer.de
Website: www.csp.fraunhofer.de